POLITECNICO DI TORINO
Repository ISTITUZIONALE

Nanoparticles production in continuous flow devices - Modelling and experimental insights into continuous flow-based processes

(Article begins on next page)

04 August 2020

ALESSIO D. LAVINO, DANIELE MARCHISIO, MARCO VANNI, ADA FERRI, ANTONELLO A. BARRESI*
*Corresponding author
Department of Applied Science and Technology, Politecnico di Torino, Italy

Nanoparticles production in continuous flow devices
Modelling and experimental insights into continuous flow-based processes

KEYWORDS: Nanoparticles, solvent displacement, flash nanoprecipitation, population balance model, molecular dynamics, computational fluid dynamics, flow chemistry.

ABSTRACT

In this work, a general overview on nanoparticles formation processes is given from both modelling and experimental points of view. The key mechanisms are presented and identified, despite some of them are still under debate. Experiments investigated the effect of different good solvents, as well as the role played by the presence of active principles, and more detailed confirmations have been found out thanks to modelling efforts. Population balance modelling and computational fluid dynamics simulations got a deeper insight into the mechanisms and the good solvent effects that lead to nanoparticles formation. Simulations results confirm the trends experimentally observed. Future investigations can be carried out by means of classical molecular dynamics, in order to gain a better understanding of the nanoparticle's formation dynamics.

INTRODUCTION

Nanoparticles formation is a complex process and numerous are the investigations, either experimental or by modelling, that have been conducted, due to the wide range of applications (e.g., pharmaceuticals, cosmetics, biology, textile industry). Different techniques can be used to synthesize nanoparticles; in particular, continuous flow-based and scalable techniques received a lot of attention in the last decades (1–3). One of the most employed methods is represented by the so-called solvent displacement (4), also known as flash nanoprecipitation. It consists in mixing a stream of good solvent, in which a solute (e.g., polymer) and the active principle are dissolved, with a bad solvent, or anti- or non-solvent, in which they are immiscible. As soon as the mixing occurs, the role of the anti-solvent is to destabilize the mixture, inducing nanoparticles formation and precipitation.

It usually takes place in very small mixers, order of magnitude of millimetres. Among the most used mixers (5), it is worthwhile mentioning the Confined Impinging Jets Mixer (CIJM) (6) and the Multi-Inlet Vortex Mixer (MIVM) (7), schematically represented in Figure 1. The main advantage of these kind of micro-mixers is their industrial scalability as well as their applicability in continuous flows (8). Examples of possible good solvents are tetrahydrofuran (THF), acetone and acetonitrile, whereas water is usually employed as anti-solvent. Due to the several phenomena involved and considering the main applications of nanoparticles

production, the identification of the key factors that control the final nanoparticles size and mean size distribution turns out to be of paramount importance.

The role played by some of them, such as the mixer geometry (hydrodynamics), mixing conditions, local species concentration and supersaturation, has been clarified with the help of Computational Fluid Dynamics (CFD) (5, 9, 10), but the effect of species concentration (and temperature) and the role of supersaturation itself is still a point of debate (11). Another point still to be addressed is represented by the role played by different good solvents and how they can control the final nanoparticle size. Experimental and modelling evidences are here reported to get a deeper insight into the latter aspects, representing a point of progress and novelty in the prediction and control of nanoparticle production, crucial feature in many fields of the current nanotechnology industry.
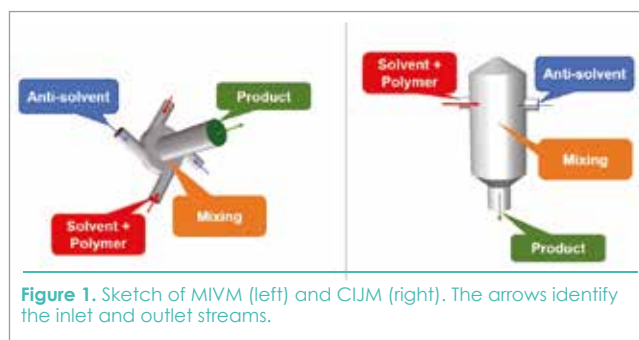
Figure 1. Sketch of MIVM (left) and CIJM (right). The arrows identify the inlet and outlet streams.

RESULTS AND DISCUSSION

Mechanisms proposed to explain nanoparticle formation
Different mechanisms have been proposed to explain the observed dependence on operating conditions: among the others, it is worthwhile to mention the classical nucleation theory, the nucleation-growth model, the nucleation-aggregation and the purely aggregative models, with possible intermediate conditions depending on the supersaturation ratio. According to nucleation-based models, an energy barrier must be overcome, whose rate is dependent on temperature and supersaturation. Growth can occur by deposition of single molecules onto the particle matrix after diffusion from the bulk, and weakly depends on the supersaturation.

Following this approach, the classical nucleation theory (10) and a modified nucleation model have been proposed to describe nanoparticles production (12).

Modelling work, based on population balance approach, has also evidenced that particle aggregation may take place in parallel to molecular growth. Aggregation is due to Brownian and turbulent fluctuations, the relative contribution depending on the initial polymer concentration (supersaturation) in good solvent stream.

The explanation of the effect of species concentration is more complex. Unfortunately, local values of supersaturation, which are those really governing the process, are difficult to evaluate experimentally, and can be estimated only by means of modelling approaches (e.g., CFD, nucleation-aggregation mechanisms (1-3)). MD simulations have confirmed that particle formation can be described by Brownian-limited aggregation of polymer molecules at high polymer concentration: the nanoparticles can be considered amorphous and no energy barrier exists for aggregation, resulting in a purely aggregative model (11, 14). The advantage and the novelty of this modelling approach consists in overcoming the usual distinction of the three different steps of nucleation, molecular growth and aggregation, by considering the molecules that form a nanoparticle as discrete building blocks, thus resulting in a purely aggregative source term, directly built upon MD simulations. Such a multiscale approach can be useful to interpret the experiments and highlight the role of the different mechanisms, recomposing some of them in a unitary vision, depending on the operating conditions (11, 15–17). Generally, at very low polymer supersaturation ratios, a purely aggregative model does not fit the experimental data well, while a nucleation-aggregation model is more effective. This kind of approach turns out to represent a valid model description of nanoparticle formation, in terms of self-assembly (7, 18, 19).

Alternatively, the "ouzo effect" (20) has been proposed to explain the initial spontaneous formation of nanoparticles by solvent displacement.
When a hydrophobic solute is rapidly brought into the metastable region between the binodal and the spinodal composition, the local supersaturation can lead to the spontaneous nucleation of small particles that subsequently grow or aggregate to form nanoparticles with a very narrow size distribution (21, 22).

Different good solvents and menthol-loaded nanoparticles
With the aim of gaining a targeted nanoparticle size, the choice of the good solvent represents also a crucial aspect. Here three different good solvents will be considered: acetone, acetonitrile and THF.
Experimental efforts (23) (filled symbols in Figure 2 and 4) clearly show that nanoparticles size decreases in the order THF>acetonitrile>acetone, inferring that the different effect of the three solvents must be explained with different intermolecular interactions between water and solvent, in terms of diffusion coefficient (23). In this analysis, menthol is firstly considered as active principle.
Being that menthol and PCL are initially dissolved in the solvent, it is reasonable to expect that water-solvent diffusivity is more relevant than the solvent-water one, since water must diffuse in the solvent to generate supersaturation.
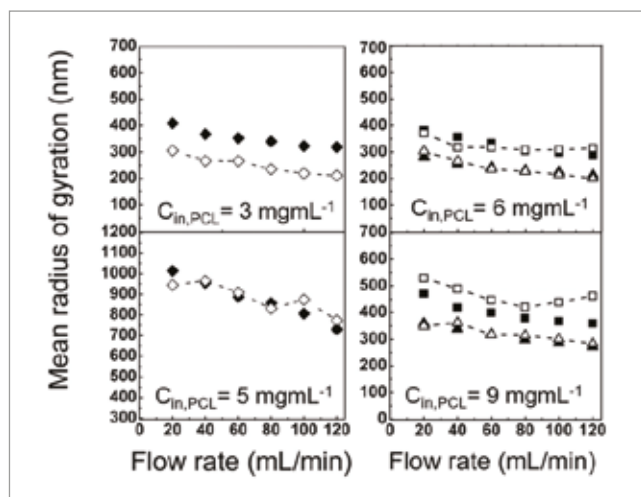
Figure 2. Mean nanoparticles size at the outlet of the CIJM, in terms of mean radius of gyration, at different inlet PCL concentration, $C_{in,PCL}$. Discrete black symbols correspond to experiments, whereas empty symbols and dashed lines are related to the purely aggregative model predictions (11). Different good solvents are considered: THF is represented on the left (diamonds, $C_{in,PCL}$=3-5 mg mL^{-1}); acetone (triangles) and acetonitrile (squares) on the right ($C_{in,PCL}$=6-9 mg mL^{-1}).

Nanoparticle size decreases in the same order as water-solvent diffusivity increases ($D_{w-acetone}$>$D_{w-acetonitrile}$>D_{w-THF}) (23), and this could be due to faster increase of supersaturation during mixing. Binary water-acetone and water-acetonitrile mixtures have been widely investigated (23–25), presenting a different behaviour: water-acetonitrile solutions are endothermic in the entire concentration range, while water-acetone solutions switch from exothermic to endothermic as the molar fraction of acetone exceeds 0.5. Significant differences in molecular interactions, resulting in different solvation structures, have been reported also between the water-acetone and the water –THF system (26).

In the case considered (the same volumes of solvent and water mixed, at equilibrium conditions) water-acetone interactions are enthalpy-controlled, forming stable clusters; on the other hand, water-acetonitrile interactions are entropy-controlled, not very strong, thus water preserves its own cluster structure, leading to a lower supersaturation and, then, to a slower nucleation forming larger nanoparticles than in acetone.

CFD simulations, by means of a purely aggregative model extensively presented and validated in (11), confirmed some of the conclusions mentioned above, founding out that a key role is played by the good solvent molar volume, as well as its solubility level. The molar volume corresponds, in turn, to a given molar fraction which the Flory's parameters functional forms are strongly dependent on, as shown in (11). The solubility is expressed in terms of Hansen solubility distances from PCL (27). It represents the ability of a solvent to solubilise a solute: the shorter the distance is, the more soluble, then compatible, that solvent is with the given solute. In line with the solubility distances from PCL (Figure 3), it is possible to show that the dimension of the single PCL molecule follows the order THF>acetone>acetonitrile, but the predicted clusters/nanoparticles are larger in acetonitrile than in acetone, because of the corresponding molar volume, which is strictly related to the molar fraction. By means of Flory's theory of real polymers, nanoparticles aggregation rate follows the

order THF>acetonitrile>acetone, justifying the different mean nanoparticles sizes (Figure 2 and 4). This is in accordance with the experimental observation of the different "mixing" behaviour, previously described.

Other key aspects are represented by the quench ratio (i.e., volume of water in the process to volume of quench water ratio), together with the polymer to active principle mass ratio, MR, in the inlet stream. Nanoparticles show larger mean size by increasing both the active principle quantity and the quench ratio (less quench water is used, more particles can aggregate).

This is clearly depicted in Figure 4, where acetone (left) and acetonitrile (right) are compared at different MR and quench ratios. Quench ratios and MR, however, are not considered by computational models, paving the way for future investigations.
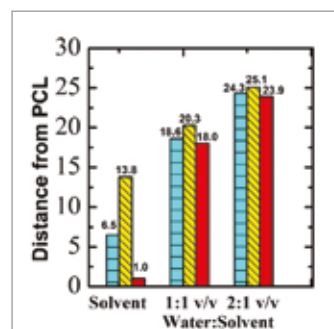
Figure 3. Hansen solubility distances from PCL for acetone (light blue, horizontally dashed), acetonitrile (yellow, diagonally dashed) and THF (red), at different proportions in volume with water. Image taken with permission from (23), modified.
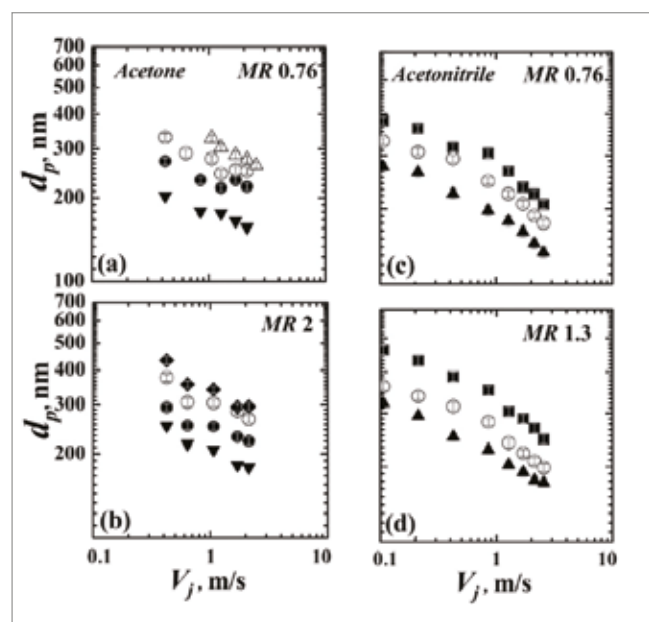
Figure 4. Effect of the inlet velocity and active principle (menthol) to PCL mass ratio (MR) in acetone (left) and acetonitrile (right). Inlet polymer concentration, C_{PCL}: ▼ , 2 mg/mL; ▲ , 3 mg/mL; ● ,4 mg/mL; ◐ , 6 mg/mL; ◆, 8 mg/mL; ■, 9 mg/mL; △ ,10 mg/mL. Image taken from (23) with permission, modified.

The most used active principles in nanoparticles formation
One of the first active principles used in the loading of nanoparticles, via solvent displacement, was represented by the doxorubicin (28), an anti-cancer compound. Other encapsulants have been tested and reported in literature: menthol, caffeine, and melatonin were proposed for both textile and transdermal applications (29). It was noticed that they only slightly affect the final nanoparticle size and its dependence on mixing conditions. When the active principle or the drug is poorly soluble in water, then it is mixed with the polymer in the solvent. It is also possible to incorporate substances that have a relatively good solubility in water, as in the case of menthol, or even those whose solubility is higher in water than in the organic solvent (caffeine), producing very interesting results in terms of incorporation and loading efficiency (30), strongly depending on the operating conditions (whether they are initially dissolved in either the good or the bad solvent).

METHODS

CFD simulations were carried out by using ANSYS Fluent 15.0, a commercial code, while MD analysis were conducted thanks to an open-source tool, GROMACS simulation package. The PCL (molecular weight of 14,000 Da) was obtained from Sigma Aldrich. Acetone, acetonitrile Chromasolv (HPLC grade), and tetrahydrofuran (THF) were also purchased by Sigma-Aldrich. A Milli-Q RG system by Millipore R (Billerica, USA) was used to produce ultrapure water employed in all experiments.

CONCLUSIONS

A broad scenario on nanoparticles production has been given, in which the key aspects that govern the solvent displacement process are underlined. Both experiments and modelling approaches are presented, showing the main mechanisms proposed to explain such a complex phenomenon. Despite from an experimental point of view several analyses have already been conducted, further insights into nanoparticles formation, in terms of role played by the different active principles and the different good solvents, can be achieved thanks to future Molecular Dynamics investigations.

REFERENCES AND NOTES

1. Horn D., Rieger J., *Ang. Chemie Int. Ed.,* 40, 4330–4361 (2001).
2. Johnson B.K., Prud'homme R.K., *AIChE J.,* 49, 2264–2282 (2003).
3. Bourne J.R., Yu S., *Ind. Eng. Chem. Res.,* 33, 41–55 (1994).
4. Fessi H., Puisieux F., et al., *Int. J. Pharm.,* 55, R1–R4 (1989).
5. Lince F., Marchisio D.L., et al., *Chem. Eng. Proc.,* 50, 356–368 (2011).
6. Lince F., Marchisio D.L., et al., *Chem. Eng. Res. Des.,* 87, 543–549 (2009).
7. Cheng J.C., Fox, R.O., *Ind. Eng. Chem. Res.,* 49, 10651–10662 (2010).
8. Valente I., Celasco E., et al., *Chem. Eng. Sci.,* 77, 217–227 (2012).
9. Liu Y., Cheng C., et al., *Chem. Eng. Sci.,* 63, 2829–2842 (2008).
10. Di Pasquale N., Marchisio D.L., et al., *Chem. Eng. Sci.,* 84, 671–683 (2012).
11. Lavino A.D., Di Pasquale N., et al., *Chem. Eng. Sci.,* 171, 485–494 (2017).
12. Di Pasquale N., Marchisio D.L., et al., *Chem. Eng. Res. Des.,* 91, 2275–2290 (2013).
13. Aubry J., Ganachaud F., et al., *Langmuir,* 25, 1970–1979 (2009).
14. Lavino A.D., Di Pasquale N., et al., *AIP Conf. Proc.,* 1695, 020036 (2015).
15. Zelenková T., Mora M.J., et al., *J. Pharm. Sci.,* 107, 1157–1166 (2018).

16. Zelenková T., Onnainty R., et al., *Europ. J. Pharm. Sci.,* 119, 135-146 (2018).
17. Zelenková T., Fissore D., et al., *J. Pharm. Sci.,* 103, 1839–1850 (2014).
18. Liu Y., Tong Z., et al., *Pest Manag. Sci.,* 64, 808–812 (2008).
19. Cheng J.C., Vigil R.D., et al., *J. Colloid Interf. Sci.,* 351, 330–342 (2010).
20. Vitale S.A., Katz J.L., *Langmuir,* 19, 4105–4110 (2003).
21. Beck-Broichsitter M., Rytting E., et al., *Europ. J. Pharm. Sci.,* 41, 244–253 (2010).
22. Ganachaud F., Katz J.L., *ChemPhysChem,* 6, 209–216 (2005).
23. Ferri A., Kumari N., et al., *Canad. J. Chem. Eng.,* 95, 1690–1706 (2017).
24. Perera A., Sokolić F., *J. Chem. Phys.,* 121, 11272–11282 (2004).
25. Lavino A.D., Banetta L., et al., *J. Phys. Chem. B,* 122, 5234–5241 (2018).
26. Katayama M., Ozutsumi, K., *J. Solution Chem.,* 37, 841–856 (2008).
27. Hansen Solubility Parameters: A User's Handbook, Edited by Hansen C.M., 2nd ed. CRC Press, Boca Raton, Florida, USA (2007).
28. Lince F., Bolognesi S., et al., *Chem. Eng. Res. Des.,* 89, 2410–2419 (2011).
29. Mossotti R., Ferri A., et al. *J. Microencapsul.,* 32, 650–660 (2015).
30. Massella D., Celasco E., et al., *Polymers,* 10, 1092 (2018). ▪

ABOUT THE AUTHORS

Alessio Lavino is a Post-Doctoral Research Assistant at Politecnico di Torino. His research focuses on the multiscale modelling of polymer self-assembly, by means of full-atom and coarse-grained Molecular Dynamics and Computational Fluid Dynamics. He accomplished a PhD in Chemical Engineering in 2019 and is very active in the area of molecular dynamics and population balance modelling with quadrature-based moments methods.

Antonello Barresi is a currently full professor of Transport phenomena at Politecnico di Torino, in charge of the course of Process development and design. His research activity, both modelling and experimental, is focused on drying and freeze-drying, mixing and production of nanostructured material for pharmaceutic applications, monitoring and control. Author of more than 250 papers and more than 100 Conference presentations.